

Computational workflows for perovskites: Case study for lanthanide manganites

P. Kraus, P. Raiteri, J. D. Gale

E-mail: peter.kraus@ceramics.tu-berlin.de

Supporting information

The open source code `mash`, used to generate starting structures of perovskites in this work, is available at <https://github.com/PeterKraus/mash>. Version 1.0, which was used in this work, is also archived under DOI: 10.5281/zenodo.7492808.

The latest version of the complete code archive including all Quantum ESPRESSO calculation input and output files, as well as postprocessing scripts used to generate the figures in this manuscript, is available on Zenodo under DOI: 10.5281/zenodo.7492855.

Supplementary tables

Table S1: Comparison of pseudopotential libraries. Effect on the root mean square deviation (RMSD) from the reference r_e for the 17 lanthanide diatomics, as well as the La-containing subset of 5 diatomics.

| DFA | Pseudopotential | RMSD of r_e (mÅ) | |
|--------|------------------|--------------------|-------|
| | | 17 LnX | 5 LaX |
| PBE | SSSP Eff. PBE | 18.4 | 22.9 |
| | SSSP Eff. PBEsol | 17.7 | 22.0 |
| | SG15 ONCV PBE | – | 43.4 |
| PBEsol | SSSP Eff. PBE | 30.6 | 6.4 |
| | SSSP Eff. PBEsol | 30.8 | 6.2 |
| | SG15 ONCV PBE | – | 11.2 |
| WC | SSSP Eff. PBE | 27.8 | 4.7 |
| | SSSP Eff. PBEsol | 27.7 | 4.2 |
| | SG15 ONCV PBE | – | 24.5 |
| N12 | SSSP Eff. PBE | 19.2 | 18.5 |
| | SSSP Eff. PBEsol | 19.7 | 19.3 |
| | SG15 ONCV PBE | – | 38.5 |

Supplementary figures

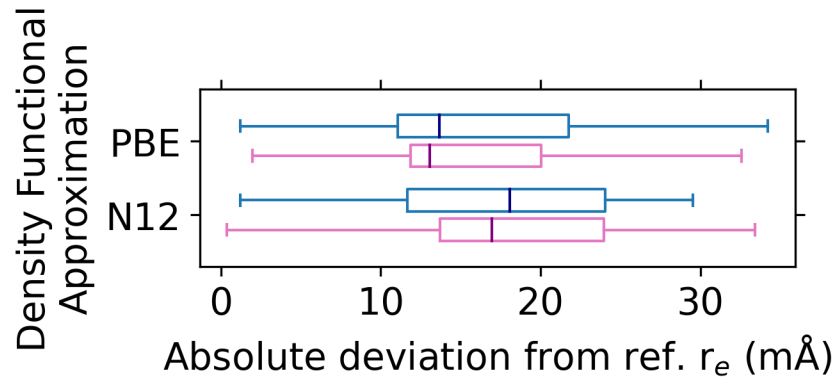


Figure S1: Comparison of the distribution of absolute deviations from reference r_e for the 17 lanthanide diatomics, obtained using a $3 \times 4 \times 3$ Monkhorst-Pack k -point grid (blue) and a Γ -point calculation with Makov-Payne correction for isolated systems (pink). With a T-test p -value of 0.93 and 0.82 for PBE and N12, respectively, the difference in the results is not statistically significant.

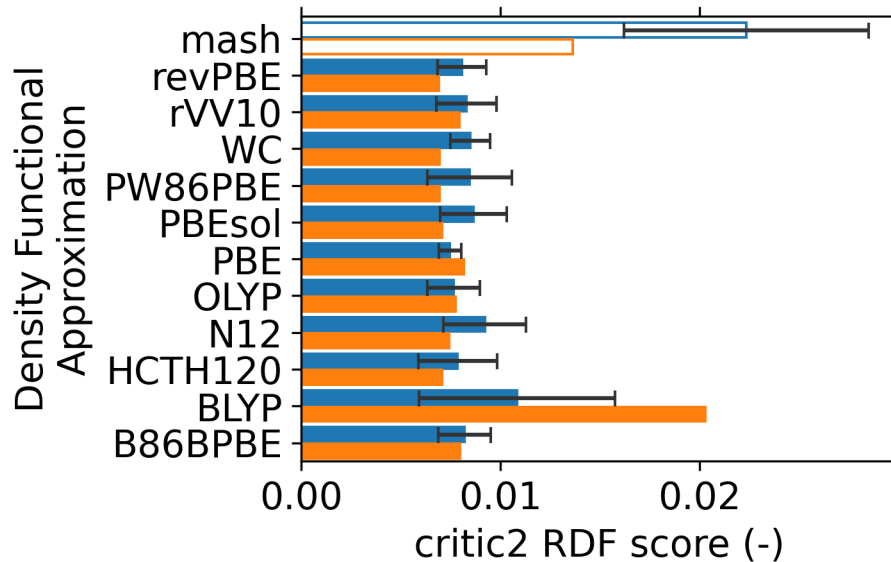


Figure S2: Dissimilarity scores calculated with the RDF method in `critic2` using computed and experimental crystal structures of lanthanide perovskites. Values obtained for the initial structures generated by `mash` included for comparison. Average score for a set of five perovskites shown in blue, standard deviation of the set indicated using error bars, and the score for the LaMnO_3 perovskite shown in orange.

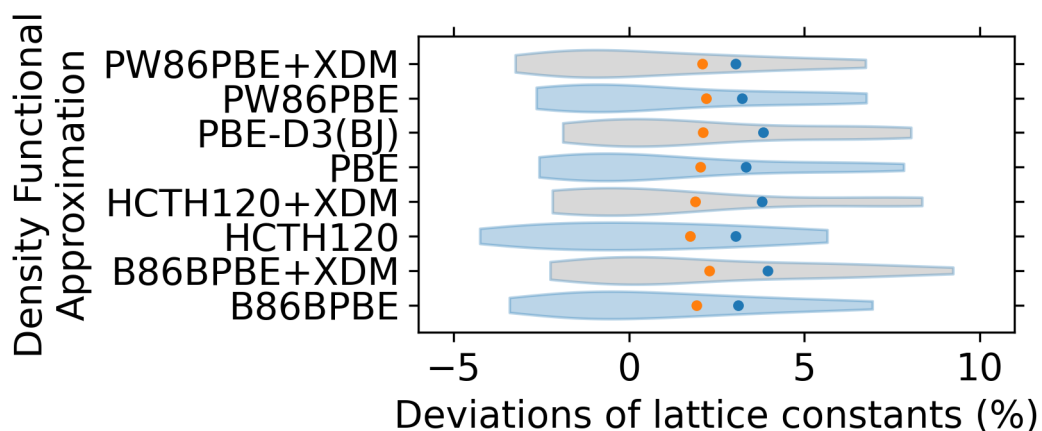


Figure S3: Effect of dispersion corrections on the performance of DFAs in predicting lattice constants of lanthanide perovskites. Violin plots show signed relative deviations from reference values. Relative RMSD for a set of five perovskites shown as blue dots, the relative RMSD for the LaMnO_3 perovskite shown as orange dots. The results for dispersion-corrected DFAs shown in grey for clarity.

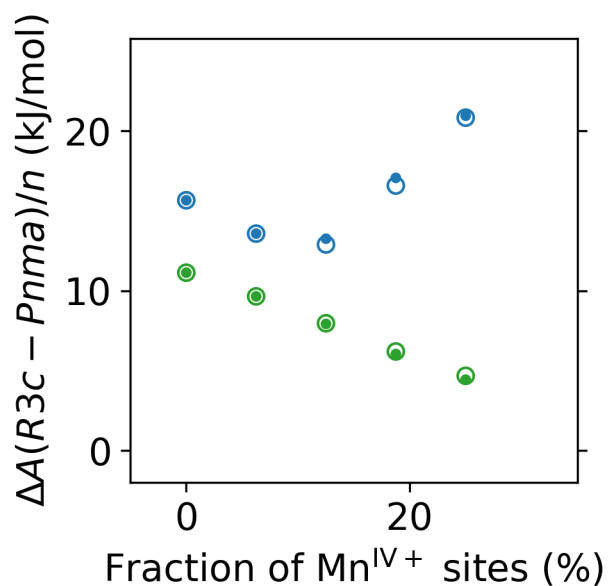


Figure S4: Difference in the Helmholtz free energies, considering the energies and weights of all evaluated structures, at 1000 K (circles). The differences in the total energies, $\Delta E(R3c - Pnma)/n$, shown for comparison (dots). Calculated with PBE+ U (blue) and HCTH120 (green).

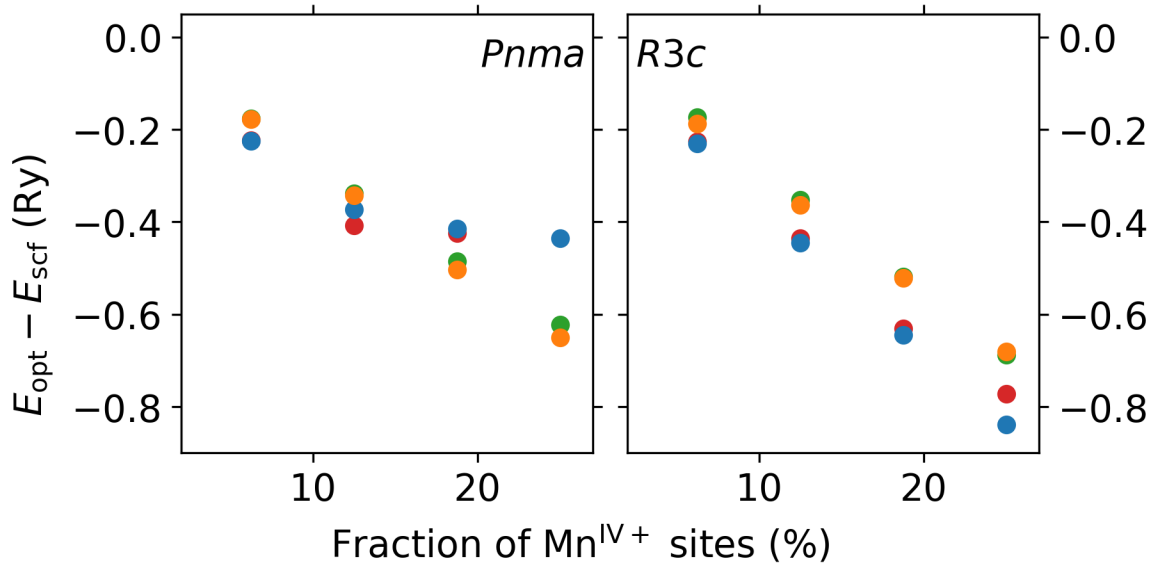


Figure S5: Cell relaxation energy for the lowest-energy *Pnma* (left) and *R3c* (right) defective supercells, calculated with PBE+*U* (blue), N12+*U* (red), HCTH120 (green), and OLYP (orange).